Moroccan Journal of Chemistry
ISSN : 2351-812X

Mor. J. Chem., 2023, Volume 11, Issue 3, Page 802-817
https://revues.imist.ma/index.php/morjchem
https://doi.org/10.48317/IMIST.PRSM/morjchem-v11i3.40986

Organic compounds based on 1-(prop-2-yn-1-ylamino)-2,3-dihydro-1H-indene-4-thiol as selective human monoamine oxidase B inhibitors. Quantitative analysis of structure-activity relationships and *in-silico* investigations

M. Ahfid El Alaouy [1, *], S. El Bahi[1], M. Boutalaka[1], M. Ouabane [1,2], A. Sbai [1,*], H. Maghat[1], M. Bouachrine [1,3], T. Lakhlifi[1]

[1] *Molecular chemistry and Natural Substances Laboratory, Faculty of Science, University Moulay Ismail, Meknes, Morocco*
[2] *Chemistry- Biologie Applied to the Environment URL CNRT 13, department of chemistry, Faculty of Science, Moulay Ismail University, Meknes, Morocco.*
[3] *EST Khenifra, Sultan Moulay Sliman University, Benimellal, Morocco*
**Corresponding author, Email address: a.sbai@umi.ac.ma*
***Corresponding author, Email address: mo.elalaouy@edu.umi.ac.ma*

Received *21 May 2023,*
Revised *29 June 2023,*
Accepted *03 July 2023*

Citation*: El Alaouy M. A., El Bahi S., Boutalaka M.* Ouabane M., Sbai A., *Tahar L., Bouachrine M., (2023) Organic compounds based on 1-(prop-2-yn-1-ylamino)-2,3-dihydro-1H-indene-4-thiol as selective human monoamine oxidase B inhibitors. Quantitative analysis of structure-activity relationships and in-silico investigations, Mor. J. Chem., 14(3), 902-817.*

Abstract: After Alzheimer's disease, Parkinson's disease is the most prevalent neurodegenerative condition. Because it is fatal and affects a large proportion of the world's population over the age of 60, the development of new drugs to treat it is crucial. To achieve this objective, we used the 3D-QSAR technique to design effective hMAO-B inhibitors from a 1-(prop-2-yn-1-ylamino)-2,3-dihydro-1H-indene-4-thiol chain. The 3D-QSAR models were generated by combining comparative molecular field analysis (CoMFA) and comparative molecular similarity index analysis (CoMSIA). In this study, the different field models obtained proved that the CoMSIA/SEA model is the best model with excellent predictive power over several models (Q^2 = 0.701; R^2 = 0.926; R^2_{test}= 0.69). A new group of MAO-B inhibitors was predicted based on this fitting model, and the pharmacokinetic properties were studied using ADMET in silico prediction. All examined compounds showed good oral bioavailability. In addition, the docking simulation of the designed compound M4 and the most active compound of the training set K12 were analyzed. The results showed that the newly designed compound M4 remained more stable at the active site of the receptor compared to the compound K12, and we can finally rely on it as a potential pharmacological compound.

Keywords: ADMET; 3D-QSAR; Molecular docking; hMAO-B.

1. Introduction

Two varieties of monoamine oxidase exist (MAO, EC 1.4.3.4): human MAO (hMAO A and hMAO B). MAO is present in small blood vessels in the brain, liver, mucosa of the gastrointestinal tract, and other organs. Monoamine neurotransmitters such as serotonin, dopamine, tyramine, norepinephrine, N-methyl-4-phenyl-1,2,3,6-tetrahydropyridine (MPTP), and flavin adenine dinucleotide are oxidatively deaminated by MAOs (Aydin *et al.*, 2020). HMAO A interacts especially with serotonin and norepinephrine. HMAO B hydrolyzes phenylethylamine monoamine (PEA) and benzylamine. Both isoforms also hydrolyze dopamine, tyramine, and tryptamine. In the presence of oxygen and water, both enzymes react with their respective amines(Aigner *et al.*, 2017), forming

aldehydes, ammonia, and one equivalent of hydrogen peroxide. MAO A and B are involved in a variety of physiological (pathological) processes in humans (Edmondson *et al*., 2009). Therefore, monoamine-related disorders such as Parkinson's disease (PD), Alzheimer's disease (AD), and depression are treated with MAO inhibitors. Inhibitors are classified according to isoform selectivity, which includes non-isoform selectivity, as well as the type of enzyme inhibition, which includes reversible and non-reversible inhibitors(Aigner *et al*., 2017). While hMAO A inhibitors such as moclobemide are used to treat depression, selective hMAO B inhibitors such as selegiline (diprenil) are used to treat Parkinson's disease. hMAO-B inhibitors are useful and effective in improving motor fluctuations in patients with (PD)in the treatment (Icht *et al*., 2022)of early to advanced PD, alone or in combination with other antiparkinsonian drugs. This family of drugs increases dopamine levels and is safer than other treatments for reducing PD symptoms(Fišar, 2016). However, concerns regarding the selectivity of these drugs have been highlighted, and side effects such as hepatotoxicity and the "cottage cheese" effect have hindered their use in medicine. A few non-selective hMAOA/hMAO-B inhibitors, such as caroxazone, have been withdrawn from the market due to potentially dangerous and unlikely side effects. In addition to Parkinson's disease, hMAO-B has been implicated in the pathogenesis of many human diseases, making it a potential target for the treatment of a wide range of conditions, including inflammation, chronic pain, muscular dystrophy, and cancer (Kong *et al*., 2021a). Concerning (PD), hMAO B inhibitors have been shown to facilitate memory formation in patients with (AD). As a result, there have been increasing efforts to develop and discover drugs that inhibit hMAO B to treat (PD) (Aigner *et al*., 2017), (AD), and memory problems, and to alleviate cognitive impairment without impairing brain function (Hawkins, 2021). The main objective of this work is to investigate the therapeutic characteristics of 27 derivatives of the compound 1-(prop-2-yn-1-ylamino)-2,3-dihydro-1H-indene-4-thiol as potent selective inhibitors of hMAO B (Awasthi *et al*., 2020).

Over the past two decades, computer-aided drug design has been an effective method for identifying new drug candidates. This new technique is a tool to reduce the time and resources required for chemical synthesis in the laboratory. In this work, carefully planned QSAR studies provided predictive models and a series of graphical contour maps (Li *et al*., 2021).

The molecular docking approach was also used to study the interactions of new drugs with protein active site residues, as well as an ADMET predictor, which is critical for the efficacy and safety of the therapeutic drug test (Aoumeur *et al*., 2021; Koubi *et al*., 2022). Finally, for the proposed results to be evaluated, the molecules must pass through all these filters (Xin *et al*., 2021). The results of this study provide essential information for the creation of new inhibitors (Sherry, 2001).

2. Material and methods

2.1 Procedure for splitting and minimizing datasets

In this research paper, we used a series of human monoamine oxidase B inhibitors from the work of Haiyan Kong et al (Kong *et al.,* 2021b). The structures of 1-(prop-2-yn-1-ylamino)-2,3-dihydro-1H-indene-4-thiol derivatives, as well as their activity levels, are shown in **Figure 1 and Table 1**. For the CoMFA and CoMSIA analyses, the inhibitory activity (IC_{50}) was transformed into negative log units and reported as pIC_{50}. In addition, the dataset was divided into two parts: the training set and the test set, which were used to generate the final 3D-QSAR models and to evaluate the predictive accuracy of these models. In addition, the test set was chosen with the following criteria in mind: the inhibitory structures in the test set should be varied, and their inhibitory actions should be similar to those in the training set (Wang *et al.,* 2021). Sybyl software was used for molecular modeling and 3D QSAR experiments. To develop a stable structure of the inhibitors, a systematic and comprehensive search was first performed.

Then, the Gasteiger-Hückel method was used to add partial atomic charges (Fu *et al.,* 2018). Then, energy reduction was performed using a Tripos force field. The convergence criterion of 0.01 kcal/mol or in 1000 minimization cycles, is all available in SYBYL (Clark *et al.,* 1989).

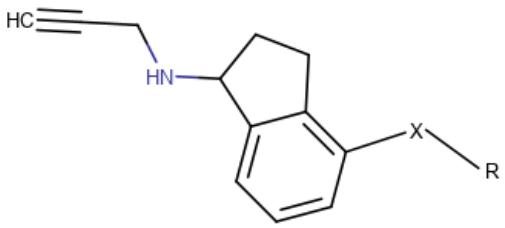

Figure 1. The formula of the studied chemical compounds.

Table 1. Activities and structures of 1-(prop-2-yn-1-ylamino)-2,3-dihydro-1H-indene-4-thiol derivatives.

N°	X	R	IC_{50} (µM)	pIC_{50}
K_1	S	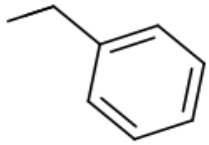	6.4	5.194
K_2	S	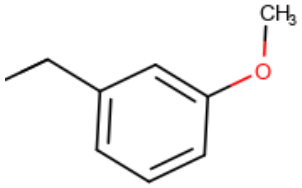	3.19	5.496
K_3	S	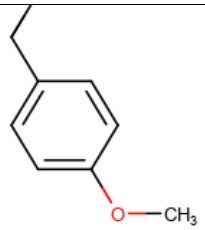	1.9	5.721
K_4	S	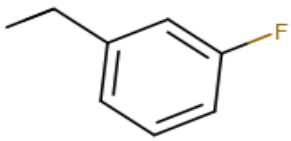	1.48	5.83
K_5	S	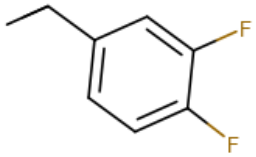	2.65	5.576
K_6	S	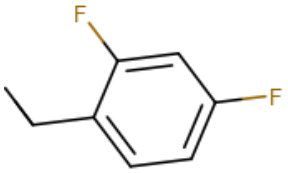	2.43	5.614

*K_7	S	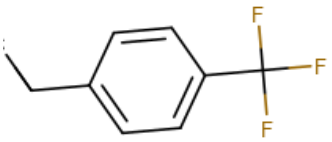	9.68	5.014
*K_8	S	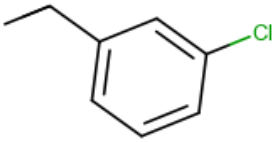	23.27	4.633
K_9	S	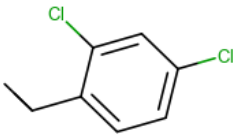	3.76	5.424
*K_{10}	S	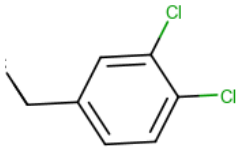	2.84	5.546
K_{11}	S		1.56	5.806
K_{12}	S	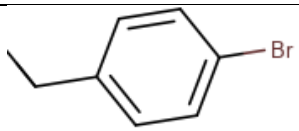	1.31	5.882
*K_{13}	S	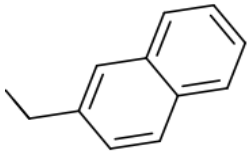	4.95	5.303
K_{14}	S	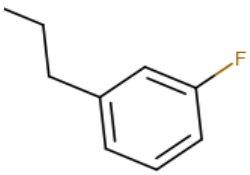	4.3	5.366
*K_{15}	S	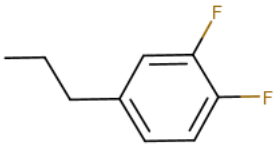	3.24	5.489
*K_{16}	S	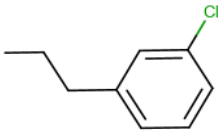	82.4	4.084

K_{17}	S	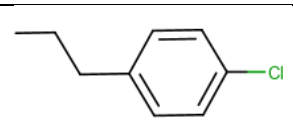	10.84	4.965
K_{18}	S	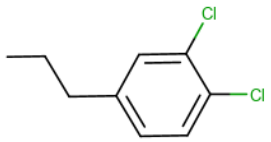	3.85	5.414
K_{19}	S	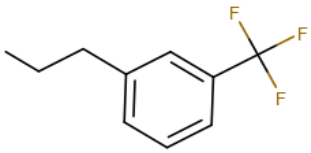	3.72	5.429
K_{20}	S	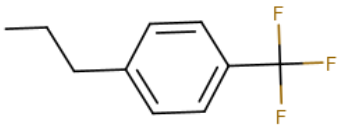	16.13	4.792
K_{21}	S	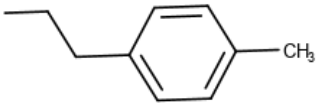	25.78	4.588
*K_{22}	S	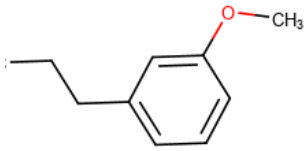	28.73	4.541
K_{23}	S	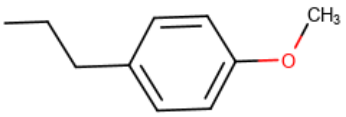	62.01	4.207
*K_{24}	S	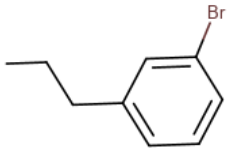	30.51	4.515
K_{25}	S	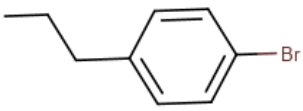	85.26	4.069
K_{26}	O	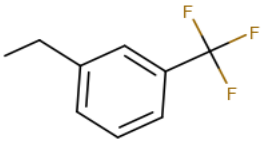	6.41	5.193
K_{27}	NH	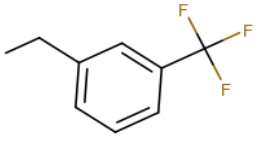	5.11	5.291

2.2 Alignment of the inhibitors

The alignment procedure is one of the most critical steps in the CoMFA and CoMSIA analysis. In this research paper, the strongest inhibitor of K12 was used as a template. The other inhibitors were aligned with the model using the "Align Database" function. The result is shown in (**Figure 2**) (Wang *et al.*, 2021).

2.3 CoMFA and CoMSIA studies

The two 3D-QSAR technologies, CoMFA and CoMSIA (Paolini *et al.*, 2019) were used in this research paper to better understand the local physical and chemical aspects of ligand-receptor interactions. Comparative Molecular Field Analysis (CoMFA) (Giansanti *et al.*, 2022) is one of the most useful 3D-QSAR approaches since its inception in 1988 (*Tabti et al.*, 2022a). A 3D cubic lattice is constructed with a mesh distance of 1 and spans 4 Å in all directions to include aligned particles.

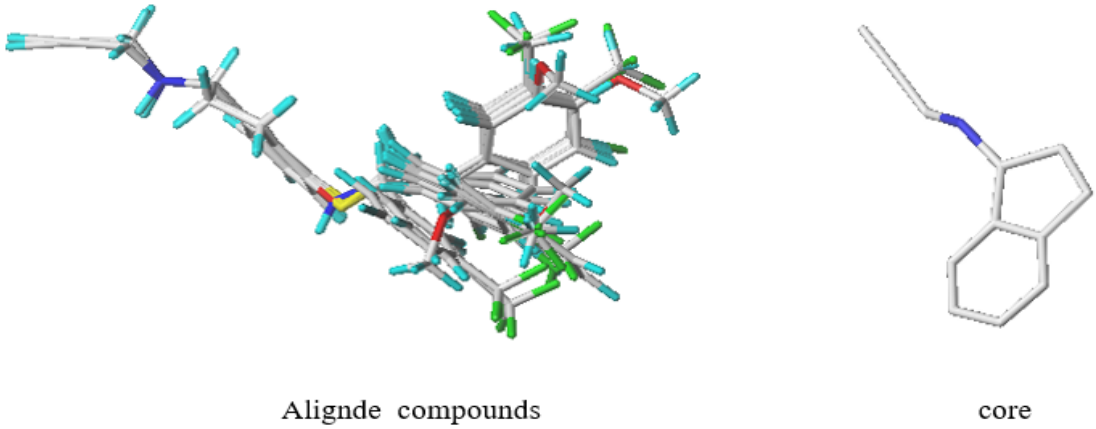

Figure 2. Overlay and alignment of the 27 molecules using Molecule K12 as a model.

CoMFA fields were generated by calculating citric field energies and electrostatic fields with a distance-dependent insulator at each grid point (Samin & Azim, 2019) using an sp3 carbon probe with a charge +1. Field (CoMSIA) Calculates the similarity indices in the region surrounding each of the previously aligned molecules in the data set (El Khatabi *et al.*, 2021). CoMSIA, like CoMFA (Shagufta *et al.*, 2007), uses a probe atom to calculate five distinct similarity index fields (steric, electrostatic, hydrophobic, hydrogen bond donor, and acceptor) (Tabti *et al.*, 2022b). The incorporation of these additional fields is not intended to increase the predictive power of the models, but to distribute distinct features to spatial locations where they are important for determining contact convergence (San Juan, 2007).

2.4 Partial least square (PLS) statistical analysis

PLS was used to generate 3D-QSAR models using CoMFA and CoMSIA descriptors as independent variables and inhibitory activities as dependent variables. Column filtration was used to filter the CoMFA and CoMSIA columns before PLS analysis. In the first step, a cross-validation analysis was performed using the Analyze (LOO) technique to determine the optimal number of components (ONC) and the coefficient of determination for cross-validation q^2 (Umair *et al.*, 2021; Kasmi *et al.*, 2022). In the second step, a cross-validation analysis was performed based on the correlation coefficient (r^2), Fisher values, and standard error of estimation (SEE), which are basic statistical properties (Wang *et al.*, 2021) .

2.5 ADMET and Drug-likeness prediction

It is believed that current or potential drugs have similar distributions of physical and chemical properties. Therefore, by evaluating the simple molecular properties of current or proposed drugs, it is possible to develop simple bases/candidates that set acceptable limits for these properties (*El Masaoudy et al.*, 2023). ADMET analysis was used, which is necessary to verify the pharmacokinetic similarities of the newly developed hMAO-B inhibitors. The electronic tool SwissADMET (Daina *et al.*, 2017), Lipinski Five Judgment, and Egan and Weber (Veber *et al.*, 2002) have been used in this context, as these bases have been used in drug similarity screening studies. Compounds and properties such as lipid susceptibility, water solubility, (BBB) permeability, cytochrome P450-1A2 (CYP1A2 enzyme), human gastrointestinal absorption (HIA), and permeability were also investigated. Skin (log Kp) and toxicity using the pkCSM web server. If a compound violates two or more rules, it may not be orally active (Pires *et al.*, 2015).

2.6 *Molecular docking*

The CB-Dock (guided blind docking for cavities detection) server (http://clab.labshare.cn/cb-dock/php/index.php; accessed February 21, 2022) was used by the researchers in this paper to analyze the structural interaction mechanisms between ligands and receptors, determine the most energetically efficient binding mode, and calculate centers and volumes using a novel Curvature-based cavity detection method. The server works in tandem with AutoDock Vina and was carefully optimized to achieve a higher success rate in the developed models (Flores-Castañón *et al.*, 2022). Only a protein file in PDB format and a ligand file in MOL^2, MOL, or SDF format were used as inputs for the analysis. Five suitable dockets are found by CB-Dock, which checks the input files after they are sent and converts them to pdbqt format using OpenBabel (O'Boyle et al., 2011). Based on the lowest value detected by Vina (Rose et al., 2018), the value with the lowest binding energy was determined.

3. Results and discussion

3.1 CoMFA analysis

The statistical results of the CoMFA model are presented in **Table 2**. Compared to the electrostatic (E) and static (S) models, the CoMFA (S + E) model has a strong ability to predict activity, and the calculated statistical parameters are as follows: Q^2 was 0.619 (>0.5), correlation coefficient (R^2) 0.994, F-value 196.82, standard error (SEE) 0.056 and 3 as the optimal number of components. The test set molecules were also consistent with the CoMFA (S + E) model, with the $R^2_{test} = 0.52$.

Table 2. Possible CoMFA results.

	Q^2	N	SEE	R^2	F	R^2_{test}
Steric (S)	0.729	4	0.047	0.996	276.64	0.38
Electrostatic (E)	0.017	2	0.303	0.813	5.425	0.48
S + E	0.619	3	0.056	0.994	196.82	0.52

3.2 CoMSIA analysis

On the statistical parameter values used throughout the development process, we chose eight models.The findings of the various ways in which the five variables were combined to create the various CoMSIA models are displayed in **Table 3**. For the (COMSIA/S + E + A) model, judging from the parameters in **Table 3**, the PLS analysis shows that Q^2 was 0.701 (>0.5), the correlation coefficient R^2 was 0.926, the F-value was 15.61, and the standard error estimate (SEE) was 0.19 with an optimal number of components of 4. The (COMSIA/S + E + A) model was also validated by external test vehicles with

R^2_{test} = 0.69. These statistical findings indicate that this model has a very strong predictive potential compared to other models. According to these results, we can say that this model is the most relevant model with strong predictive power and can provide important statistical keys to predict human monoamine oxidase B inhibitors. The actual and predicted activities of the CoMFA/S+E and COMSIA/S+E+A models of hMAO-B inhibitors are presented in **Table 4**.

Table 3. The different possibilities of combining fields (COMSIA/S+E+A).

	Q^2	N	SEE	R^2	F	R^2_{test}
S	0.643	3	0.176	0.936	18.42	0.499
E	0.608	2	0.223	0.898	11.025	0.716
S+E	O.669	3	0.219	0.902	11.469	0.686
H	0.608	7	0.145	0.957	27.94	0.25
H+S+E	0.606	3	0.129	0.966	35.47	0.42
S+E+A	**0.701**	**4**	**0 .19**	**0.926**	**15.61**	**0.69**
S+A	0.716	4	0.187	0.928	16.77	0.54
A+E	0.642	4	0.199	0.919	14.21	0.42

Table 4. Experimental and predicted pIC_{50} of the CoMFA/$S + E$ and CoMSIA/$S + E + A$ models

N°	pIC_{50} (M)	*CoMFA/SE*		*CoMSIA/SEA*	
		Predicted	*Residuals*	*Predicted*	*Residuals*
K_1	5.194	5.191	0.003	5.165	0.029
K_2	5.496	5.517	-0.021	5.401	0.095
K_3	5.721	5.733	-0.012	5.732	-0.011
K_4	5.83	5.871	-0.041	5.767	0.063
K_5	5.576	5.556	0.02	5.589	-0.013
K_6	5.614	5.603	0.011	5.567	0.047
***K_7**	5.014	5.759	-0.745	5.385	-0.371
***K_8**	4.633	5.929	-1.296	5.962	-1.329
K_9	5.424	5.386	0.038	5.412	0.012
***K_{10}**	5.546	5.677	-0.131	5.814	-0.268
K_{11}	5.806	5.88	-0.074	5.969	-0.163
K_{12}	5.882	5.817	0.065	5.878	0.004
***K_{13}**	5.303	5.856	-0.553	6.016	-0.713
K_{14}	5.366	5.357	0.009	5.522	-0.156
***K_{15}**	5.489	5.666	-0.177	5.884	-0.395
***K_{16}**	4.084	5.255	-1.171	5.008	-0.924
K_{17}	4.965	4.99	-0.025	4.84	0.125
K_{18}	5.414	5.391	0.023	5.178	0.236
K_{19}	5.429	5.43	-0.001	5.356	0.073
K_{20}	4.792	4.788	0.004	4.865	-0.073
K_{21}	4.588	4.516	0.072	4.528	0.06
***K_{22}**	4.541	4.125	0.416	4.661	-0.12
K_{23}	4.207	4.197	0.01	4.092	0.115
***K_{24}**	4.515	3.885	0.63	4.438	0.077
K_{25}	4.069	4.153	-0.084	4.505	-0.436
K_{26}	5.193	5.151	0.042	5.142	0.051
K_{27}	5.291	5.33	-0.039	5.349	-0.058

3.3 Y -randomization test

To avoid random association, we performed random operations on the training set compounds and evaluated the power of the model by performing ten tests in different ways. **Table 5** shows the low

values of Q^2cv (LOO) (rand) and R^2rand. The results confirm that the obtained model is not due to a random association.

3.4 Interpretation of model CoMSIA contour

The 3D fields of the best model (COMSIA/S+E+A) for the most active compound are shown in **Figure 3.** The steric field (A): Green colors indicate a favorable bulky group while yellow colors indicate an unfavorable bulky group to increase activity. There is a large green contour map near the meta and ortho substituents, which means that the addition of a bulky group (large substituents) at this position increases the biochemical activity, this can be explained by the higher activity of compound K2 (pIC_{50}=5.496) with the -OCH_3 radical in the meta position compared to compound K8(pIC_{50}=4.633) with the -Cl radical in the same position.

Table 5. Values of randomization test results

Model	R	R^2	Q^2
Original	**0.844**	**0.713**	**0.556**
Random 1	0.432	0.187	-0.448
Random 2	0.235	0.055	-0.869
Random 3	0.422	0.178	-0.775
Random 4	0.334	0.111	-0.763
Random 5	0.766	0.587	0.196
Random 6	0.572	0.327	-0.172
Random 7	0.468	0.219	-0.835
Random 8	0.330	0.109	-2.180
Random 9	0.419	0.175	-0.492
Random 10	0.496	0.246	-0.310
Random Models Parameters			
Average	0.447	0.219	-0.665

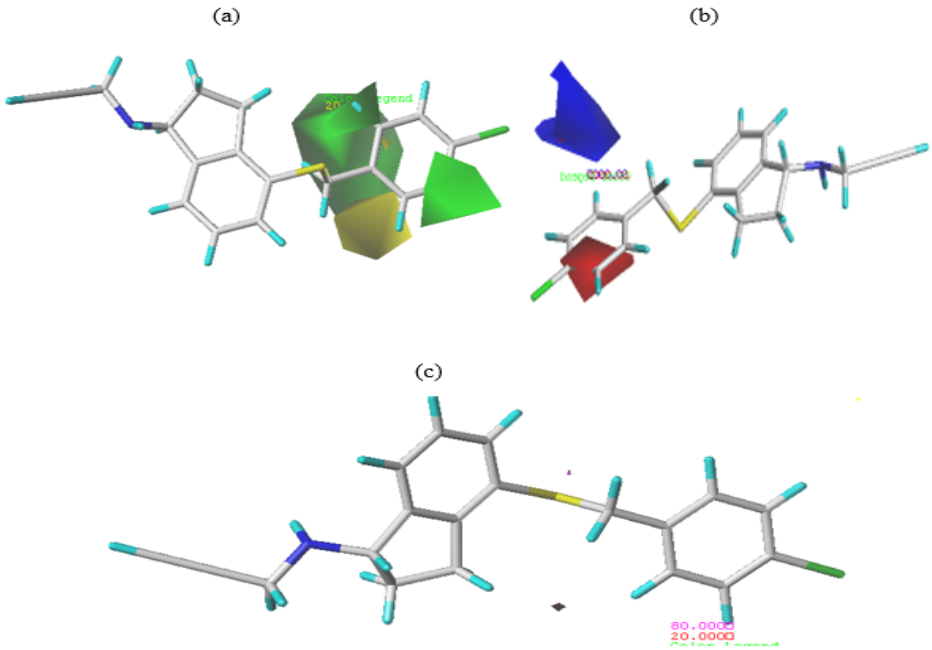

Figure 3. CoMSIA model contour map results. (a) Steric field, (b) electrostatic field, (c) hydrogen bond acceptors field

Moreover, the ortho and meta position is more efficient than the para position, which explains the higher activity of compound K19 with the -CF_3 root compared to that of compound K20 with the same root in the meta position and similarly for compound K22 with the -O-CH3 root compared to that of

compound K23 with the same root-O-CH3 in the meta position. Field (B): electrostatic contours where the blue areas are favorable to positive charges and the red areas to negative charges(Abdullahi *et al.*, 2022). We noticed a red contour next to the R substitution in the para position, indicating that the introduction of highly electronegative groups or atoms such as the halogens -Cl, -Br, and -F could increase their activity. This is illustrated by the observation that compound K17(pIC_{50}=4.965) with -Cl in the para position shows higher activity than compound K25(pIC_{50}=4.069) with -Br in the same position. Field (C): Magenta regions (80% contribution) indicate desired hydrogen bond acceptor sites, while red regions (20% contribution) indicate unwanted acceptors.

3.5 Newly designed compounds

In this work, key factors influencing inhibitory activity were identified, and substitutions were fitted to appropriate regions using the best contour mapping model (COMSIA/S+E+A) to predict novel compounds with significant activity.

Table 6. The structures and their predicted pIC_{50} of the newly developed inhibitors by the model (COMSIA/S+E+A)

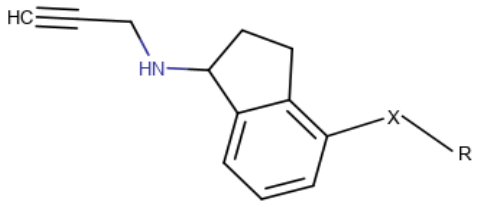

	X	R	pIC50(Pred) CoMSIA/SEA
M_1	S	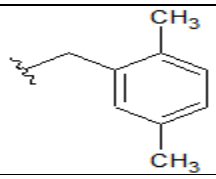	6.005
M_2	C	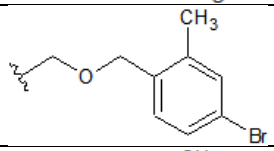	7.904
M_3	C	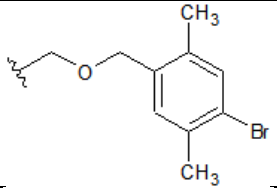	8.052
M_4	C	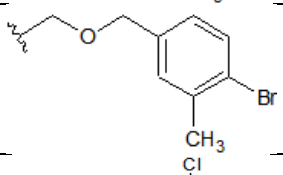	8.055
M_5	O	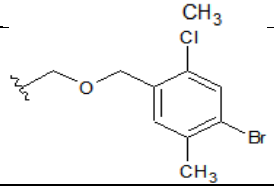	7.863

M_6	O C	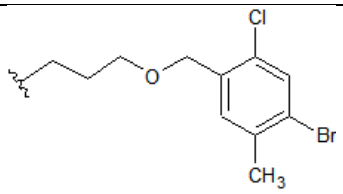	7.459
M_7	C	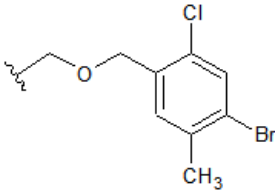	8.24

3.6 Analysis of drug-likeness and in-silico ADMET prediction

All new candidate compounds M1, M2, M3, M4, M5, M6, and M7 were shown to meet Lipinski's rule of five for oral bioavailability. In addition, the MW and logS values of all proposed molecules indicate that they have satisfactory adsorption capacity and are moderately soluble in water. In addition, all molecules showed excellent compatibility with the most important drug similarity rules, except for molecules M3, M5, M6, and M7, which have poor similarity with the drug similarity rules due to a slight increase in the logP value to some extent. Lipinski, Ghose, Veber, Egan, Muegge and showed a score of 55%, indicating good bioavailability(Khamouli *et al.*, 2022). This indicates that these substances have strong drug-like properties. All the newly generated compounds obtained a synthetic access score between 3.49 and 3.75, which means that these compounds can be easily synthesized (**Table 7**).

Table 7. Prediction of drug similarity and bioavailability of the newly designed compounds.

Compounds	Lipinski	Ghose	Veber	Egan	Alerts PAINS	Alerts Brenk	Lead likeness	Bioavailability score	Synthetic Accessibility
M1	Yes	Yes	Yes	Yes	0	1	1	0.55	3.59
M2	Yes	Yes	Yes	Yes	0	1	2	0.55	3.52
M3	Yes	Yes	Yes	Yes	0	1	2	0.55	3.68
M4	Yes	Yes	Yes	Yes	0	1	2	0.55	3.49
M5	Yes	Yes	Yes	Yes	0	2	2	0.55	3.61
M6	Yes	Yes	Yes	Yes	0	1	3	0.55	3.75
M7	Yes	Yes	Yes	Yes	0	1	2	0.55	3.58

The solubility and absorption of a drug, for example, is a critical physical and chemical property that influences whether it can be a successful therapeutic candidate. Molecular weight (MW) (≤500Da), polarity (TPSA < 140 A^2), elasticity (0 < volatility < 9) and logP less than 5. In contrast, molecules with the total polar area (TPSA) <140 °C Rotational bonds (NROTB) <10, show good bioavailability. **Table 8** lists the physical and chemical characteristics of the novel compounds.

Table 8. Lipinski properties of newly designed inhibitors.

	Log P	HBD	HBA	TPSA	Nrotb	MR	MW
M1	4.805	1	1	37.33	5	100.59	321.489
M2	4.72	1	2	21.26	7	107.27	398.34
M3	5.42	1	2	21.26	7	112.24	412.36
M4	4.726	1	2	21.26	7	107.27	398.34
M5	5.174	1	3	21.26	7	109.0	434.75
M6	5.606	1	3	30.49	9	118.61	462.81
M7	5.30	1	2	21.26	7	112.28	432.78

From the results of ADMET (**Table 9**), it appears that all chemicals are less permeable to Kp. The gastro-intestinal index (GI), which is reported as high and indicates that all substances are highly absorbed in intestinal HIA, explains the absorption of the molecule in the gut. To treat Parkinson's disease, we need to focus on drug permeability across the blood-brain barrier (BBB) (Khamouli *et al.*, 2022)whose main function is to restrict the passage of most compounds from the blood into the brain. This is important for the design of drugs that cross the BBB. It has been predicted that all compounds cross the blood-brain barrier (BBB) and thus may be suitable for the treatment of Parkinson's disease. P-glycoprotein (P-gp), it is a drug flow vector that transports toxins and vital foreign substances away from cells, and acts as a biological barrier to protect cells from the negative effects of drugs. In addition, all compounds are a substrate for P-gp, because it alone metabolizes 50% of all medications, CYP3A4 was the most significant enzyme within the CYP enzyme family. In addition, the negative AMES toxicity test also indicates that the studied derivatives (M1, M2, M3, M4, M5, M6, and M7) are not toxic.

Table 9. ADMET prediction of the newly designed compounds.

Comp	GI Absorption	BBB permeant	log kp (cm/s)	P-gp substrate	CYP1A2 inhibitor	CYP2C19 inhibitor	CYP2C9 inhibitor	CYP2D6 inhibitor	CYP3A4 inhibitor	AMES toxicity
M1	High	Yes	-5.02	Yes	No	Yes	Yes	Yes	Yes	No
M2	High	Yes	-5.54	Yes	No	Yes	No	Yes	Yes	No
M3	High	Yes	-5.36	Yes	No	Yes	No	Yes	Yes	No
M4	High	Yes	-5.54	Yes	No	Yes	No	Yes	Yes	No
M5	High	Yes	-5.45	Yes	No	No	Yes	Yes	Yes	No
M6	High	Yes	-5.44	Yes	No	No	No	Yes	Yes	No
M7	High	Yes	-5.30	Yes	No	Yes	Yes	Yes	Yes	No

3.7 Docking results

Information on the structural basis and potential interactions between the derivative and receptor binding was gathered by a molecular docking study. We need to determine the active site of human monoamine oxidase hMAO B before we can further investigate the mode and type of interactions in the different complexe. The MAO B substrate binding site is predominantly hydrophobic, surrounded by aromatic and aliphatic residues, except for a conserved lysine (Lys296) that reacts with a water molecule. MAO B tyrosines 398 and 435 are located on opposite sides of the inhibitors and substrates. MAO B tyrosines 398 and 435 are located on opposite sides of the inhibitors and substrates. The covalent bonds between this residue and MAO-B allow the formation of an aromatic "sandwich", which stabilizes the bond with the substrate. There is a small hydrophobic cavity next to the substrate cavity surrounded by residues Phe103, Pro104, Trp119, Leu164, Leu167, Phe168, Leu171, Ile199, Ile 316, and Tyr326. The second cavity is also located between the active site and the surface of the protein(A. Sbai, 2022). The following residues (Tyr326, Ile199, Leu171, and Phe168) form the boundary between the insertion cavity and the "substrate cavity," and their position affects the substrates and inhibitors capable of binding to MAO-B(Prilusky *et al.*, 2011). **Figure 4** and **Figure 5** show the results of the molecular docking reaction modes between Receptor for Human Monoamine Oxidase (PDB: 2XFQ) and the most active K12 molecule and the proposed M4 molecule. Compound K12 exhibits alkyl interactions with residues Ile316 (4.79 Å), Ile199 (3.96 Å), Ile198 (5.1 Å), Cys172 (4.92 Å) and Leu171(4.82 Å). Carbon-hydrogen interaction with residues Ile199 (3.26 Å), Pi-sigma interaction with residue Leu171(3, 94 Å), Pi-alkyl interaction with residue Tyr326 (5.35 Å), Pi-hydrogen-bond-donor interaction with residue Gln206(3.56 Å), and Pi-Pi stacked interaction with residue Tyr398 (3.89 Å) (Aoumeur *et al.*, 2021).

The proposed chemical compound M4 displays a conventional hydrogen bonding interaction with the Ile199 (2.7 Å) residue, as shown in **Figure 4**. Pi-alkyl interaction with residues Tyr326(4.57 Å) and Tyr398(4.65 Å). Alkyl interaction with residues Ile316 (3.80 Å), Leu167 (5.49 Å), Leu171 (5.04 Å), Pro104 (4.66 Å), Leu171 (4.19Å), Cys172 (4.81 Å), Cys397 (4.5 Å), and Arg42 (4.28 Å). Carbon-hydrogen interaction with the Tyr435(3.35 Å) residue.

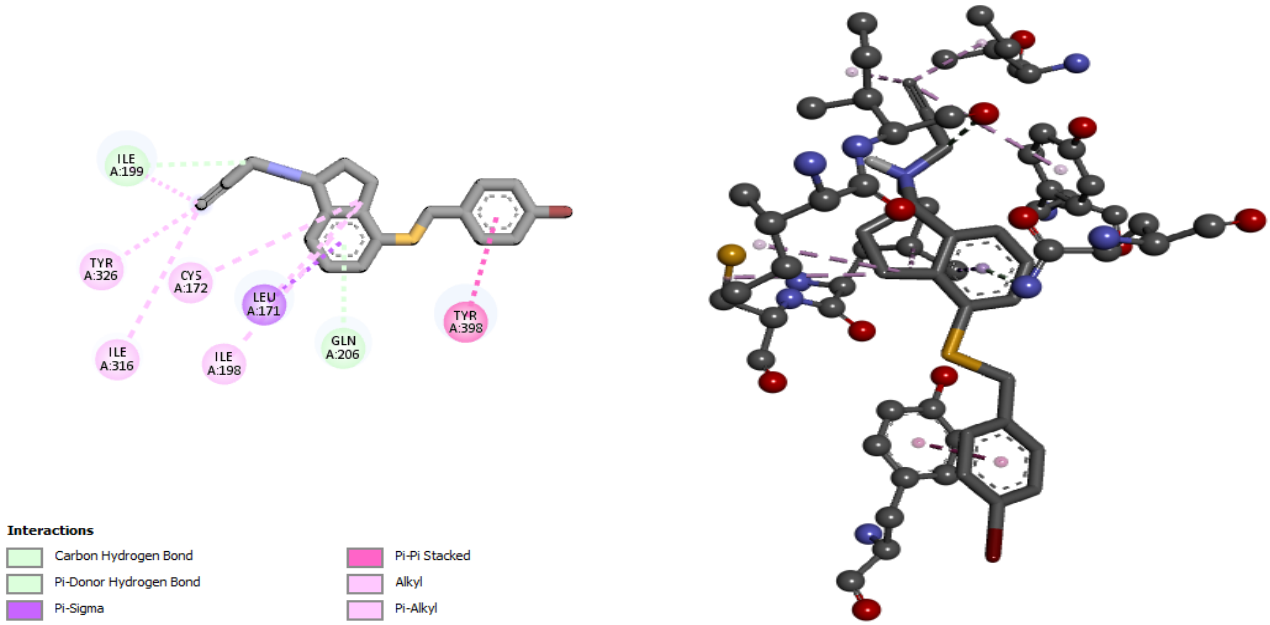

Figure 4. The chemical interactions of K12 compounds at receptor binding sites in 2D and 3D docking.

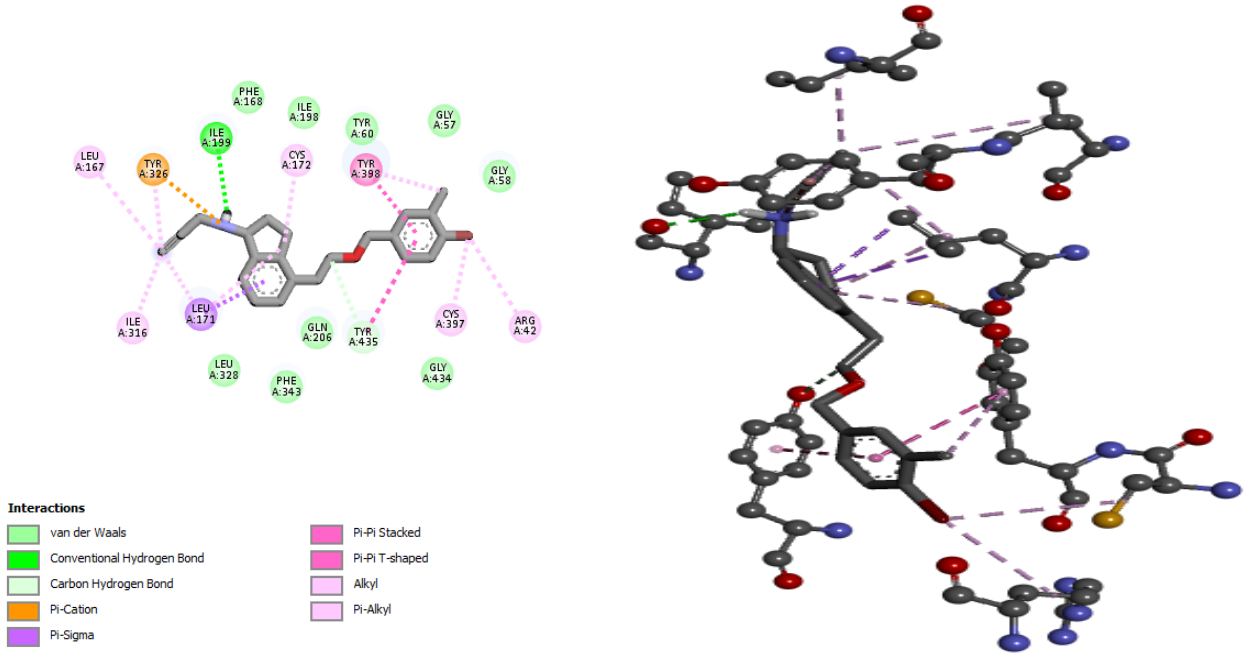

Figure 5. The chemical interactions of M4 compounds at receptor binding sites in 2D and 3D docking.

Interaction of the Pi cation with the Tyr326(4.08 Å) residue. Interaction of the hydrogen bond donor Pi- with the Gln206(3.49 Å) residue. Interaction of Pi-Pi stacked with the Leu177(3.83 Å) residue. Interaction of Pi-sigma with the Tyr398 residue (4.42 Å) and interaction of Pi-Pi shopped with the Tyr435 residue (5.58 Å). We conclude from these results that compound M4 is characterized by a large number of interactions compared to the more active compound K12 in the training set and let us not forget that the interactions between classical hydrogen bonds have a significant impact on the stability

of molecules, thus, based on these results, we conclude that compound M4 is more active in the active pocket (Bouachrine, 2020). Finally, these results support the 3D-QSAR analysis, which means that these new derivatives are more active and efficient.

Conclusion

To generate new candidates for human monoamine oxidase B inhibitors, the researchers performed computational studies (3DQSAR, molecular stabilization, MD, and ADMET simulations), using PLS analysis to predict 1-(prop-2-yn-1-ylamino)-2,3-dimers Hydro-1H-indene-4-thiol as hMAO-B inhibitors (Awasthi et al., 2020). The statistical results showed a high probability of internal and external validation with remarkable statistical power. Then, the best models obtained were tested internally and externally(Apablaza *et al.*, 2017). According to the criteria of PLS analysis, the best model (COMSIA/S + E +A) was selected (Q^2 = **0.701**, R^2 = **0.926**, R^2_{test} = **0.69**) and the contour maps also provided important information to suggest new inhibitors with better biological efficacy(Bourass *et al.*, 2016). These newly designed molecules were predicted to be orally bioavailable and a good indicator of intestinal absorption of HIA by considering different drug similarity rules (Lipinski, Weber, Ghose, Egan, ADMET prediction), and all newly designed compounds are non-toxic and cross the blood-brain barrier BBB, and docking processes were also considered in the current study, and the newly developed compound M4 participates in a classical hydrogen bonding interaction with ILE A: 199 (Awasthi *et al.*, 2020), playing an important role in the stability of the compound. Thus, the findings of this study can offer an impetus for the progress of hMAO-B inhibitors that can be used to treat Parkinson's disease.

References

Abdullahi M., Uzairu A., Shallangwa G. A., Mamza P. A., & Ibrahim M. T. (2022) Computational modelling studies of some 1,3-thiazine derivatives as anti-influenza inhibitors targeting H1N1 neuraminidase via 2D-QSAR, 3D-QSAR, molecular docking, and ADMET predictions. *Beni-Suef University Journal of Basic and Applied Sciences*, 11(1), 104. https://doi.org/10.1186/s43088-022-00280-6

Aigner M., Preissegger P., Kalcher K., Mehmeti E., Macheroux P., Edmondson D., & Ortner A. (2017) Biosensor for the characterisation of hMAO B inhibitors and the quantification of selegiline. *Talanta*, 174, 696–702. https://doi.org/10.1016/j.talanta.2017.06.079

Aoumeur N., Belaidi S., Tchouar N., Ouassaf M., Lanez T., Chtita S. (2021). Molecular docking studies for the identifications of novel antimicrobial compounds targeting of staphylococcus aureus, *Mor. J. Chem.* 9 N°1, 274-289, doi.org/10.48317/IMIST.PRSM/MORJCHEM-V9I2.19884

Apablaza G., Montoya L., Morales-Verdejo C., Mellado M., Cuellar M., Lagos C., Soto-Delgado J., Chung H., Pessoa-Mahana C., & Mella J. (2017) 2D-QSAR and 3D-QSAR/CoMSIA Studies on a Series of (R)-2-((2-(1H-Indol-2-yl)ethyl)amino)-1-Phenylethan-1-ol with Human β3-Adrenergic Activity. *Molecules*, 22(3), 404. https://doi.org/10.3390/molecules22030404

Awasthi R., Pal R., Singh P., Nagori A., Reddy S., Gulati A., Kumaraguru P., & Sethi T. (2020) CovidNLP: A Web Application for Distilling Systemic Implications of COVID-19 Pandemic with Natural Language Processing [Preprint]. *Health Informatics*. https://doi.org/10.1101/2020.04.25.20079129

Aydin T., Akincioglu H., Gumustas M., Gulcin I., Kazaz C., & Cakir A. (2020) human monoamine oxidase (h MAO) A and h MAO B inhibitors from Artemisia dracunculus L. herniarin and skimmin: Human mononamine oxidase A and B inhibitors from A. dracunculus L. *Zeitschrift Für Naturforschung C*, 75(11–12), 459–466. https://doi.org/10.1515/znc-2019-0227

Bouachrine M., Lakhlifi T. (2020) Combined 3D-QSAR Modeling and Molecular Docking Study on metronidazole-triazole-styryl hybrids as antiamoebic activity. *Moroccan Journal of Chemistry*, 8, 527-539. https://doi.org/10.48317/IMIST.PRSM/MORJCHEM-V8I2.19099

Bourass M., El Ghalia H., Ouammou A., & Bouachrine M. (2016) 3D-QSAR Models to Predict the Antiviral Activities of a series of novel N-phenylbenzamideand N-phenylacetophenone compounds based on density functional theory using statistical methods. *Moroccan Journal of Chemistry, 4,* 204-214. https://doi.org/10.48317/IMIST.PRSM/MORJCHEM-V4I1.4188

Clark M., Cramer R. D., & Van Opdenbosch N. (1989) Validation of the general purpose tripos 5.2 force field. *Journal of Computational Chemistry*, 10(8), 982–1012. https://doi.org/10.1002/jcc.540100804

Daina A., Michielin O., & Zoete V. (2017) SwissADME: A free web tool to evaluate pharmacokinetics, drug-likeness and medicinal chemistry friendliness of small molecules. *Scientific Reports*, 7(1), 42717. https://doi.org/10.1038/srep42717

Edmondson D. E., Binda C., Wang J., Upadhyay A. K., & Mattevi A. (2009) Molecular and Mechanistic Properties of the Membrane-Bound Mitochondrial Monoamine Oxidases. *Biochemistry*, 48(20), 4220–4230. https://doi.org/10.1021/bi900413g

El Khatabi K., Aanouz I., El-Mernissi R., Khaldan A., Ajana M., Bouachrine M., & Lakhlifi T. (2021) In silico analysis of 3D QSAR and Molecular Docking studies to discover new thiadiazole-thiazolone derivatives as mitotic kinesin Eg5 inhibition. *Moroccan Journal of Chemistry*, 9, 2. https://doi.org/10.48317/IMIST.PRSM/MORJCHEM-V9I2.18721

El Masaoudy Y., Tabti K., Koubi Y., Maghat H., Lakhlifi T., Bouachrine M. (2023) *I*n silico design of new pyrimidine-2,4-dione derivatives as promising inhibitors for HIV Reverse Transcriptase-associated RNase H using 2D-QSAR modeling and (ADME/Tox) properties. *Moroccan Journal of Chemistry*, 11, 300-317. https://doi.org/10.48317/IMIST.PRSM/morjchem-v11i2.35455.

Fišar Z. (2016) Drugs related to monoamine oxidase activity. *Progress in Neuro-Psychopharmacology and Biological Psychiatry*, 69, 112–124. https://doi.org/10.1016/j.pnpbp.2016.02.012

Flores-Castañón N., Sarkar S., & Banerjee A. (2022) Structural, functional, and molecular docking analyses of microbial cutinase enzymes against polyurethane monomers. *Journal of Hazardous Materials Letters*, 3, 100063. https://doi.org/10.1016/j.hazl.2022.100063

Fu Y., Sun Y.-N., Cao H.-F., Yi K.-H., Zhao L.-X., Li J.-Z., & Ye F. (2018) New Research for Quinazoline-2,4-diones as HPPD Inhibitors Based on 2D-MLR and 3D-QSAR Models. *Combinatorial Chemistry & High Throughput Screening,* 20(9), 748–759. https://doi.org/10.2174/1386207320666170622073738

Giansanti D., Pirrera A., & Meli P. (2022) The Accessibility and the Digital Divide in the Apps during the COVID-19. Comment on Cao et al. The Impact of Using mHealth Apps on Improving Public Health Satisfaction during the COVID-19 Pandemic: A Digital Content Value Chain Perspective. *Healthcare*, 10(7), 1252. https://doi.org/10.3390/healthcare10071252

Hawkins J.A. (2021) The Discovery and Implications of Neuroplasticity. In J. A. Hawkins, Brain Plasticity and Learning. *Springer International Publishing* ,1–36. https://doi.org/10.1007/978-3-030-83530-9_1

Icht M., Bergerzon-Bitton O., & Ben-David B. M. (2022) Validation and cross-linguistic adaptation of the Frenchay Dysarthria Assessment (FDA-2) speech intelligibility tests: Hebrew version. *International Journal of Language & Communication Disorders*, 57(5), 1023–1049. https://doi.org/10.1111/1460-6984.12737

Kasmi R. Bouachrine M., Ouammou A. (2022) Combined 3D-QSAR and Molecular Docking Analysis of Styrylquinoline Derivatives as Potent anti-cancer Agents, *Physical Chemistry Research* 10(3), 345-362

Khamouli S., Belaidi S., Ouassaf M., Lanez T., Belaaouad S., & Chtita S. (2022) Multi-combined 3D-QSAR, docking molecular and ADMET prediction of 5-azaindazole derivatives as LRRK2 tyrosine kinase inhibitors. *Journal of Biomolecular Structure and Dynamics*, 40(3), 1285–1298. doi.org/10.1080/07391102.2020.1824815

Kong H., Meng X., Hou R., Yang X., Han J., Xie Z., Duan Y., & Liao C. (2021) Novel 1-(prop-2-yn-1-ylamino)-2,3-dihydro-1H-indene-4-thiol derivatives as potent selective human monoamine oxidase B inhibitors: Design, SAR development, and biological evaluation. *Bioorganic & Medicinal Chemistry Letters*, 43, 128051. https://doi.org/10.1016/j.bmcl.2021.128051

Kong H., Meng X., Hou R., Yang X., Han J., Xie Z., Duan Y., & Liao C. (2021) Novel 1-(prop-2-yn-1-ylamino)-2,3-dihydro-1H-indene-4-thiol derivatives as potent selective human monoamine oxidase B inhibitors: Design, SAR development, and biological evaluation. *Bioorganic & Medicinal Chemistry Letters*, 43, 128051. https://doi.org/10.1016/j.bmcl.2021.128051

Koubi Y., Hajji H., Moukhliss Y., El Khatabi K., El Masaoudy Y., Maghat H., Ajana A., Bouachrine M., Lakhlifi T. (2022). in silico studies of 1,4-disubstituted 1,2,3-triazole with amide functionality antimicrobial evaluation against Escherichia coli using 3D-QSAR, molecular docking, and ADMET properties, *Mor. J. Chem.*, 10, 689-702, https://doi.org/10.48317/IMIST.PRSM/morjchem-v10i4.34292

Li T., Pang W., Wang J., Zhao Z., zhang X., & Cheng L. (2021) Docking-based 3D-QSAR, molecular dynamics simulation studies and virtual screening of novel ONC201 analogues targeting Mitochondrial ClpP. *Journal of Molecular Structure*, 1245, 131025. https://doi.org/10.1016/j.molstruc.2021.131025

O'Boyle N. M., Banck M., James C.A., Morley C., Vandermeersch T., Hutchison G. R. (2011) Open Babel: An open chemical toolbox. *Journal of Cheminformatics*, 3(1), 33. https://doi.org/10.1186/1758-2946-3-33
Paolini L., Piccolo M., & Zorzi M. (2019) QPCF: Higher-Order Languages and Quantum Circuits. *Journal of Automated Reasoning*, 63(4), 941–966. https://doi.org/10.1007/s10817-019-09518-y
Pires D. E. V., Blundell T. L., & Ascher D. B. (2015) pkCSM: Predicting Small-Molecule Pharmacokinetic and Toxicity Properties Using Graph-Based Signatures. *Journal of Medicinal Chemistry*, 58(9), 4066–4072. https://doi.org/10.1021/acs.jmedchem.5b00104
Prilusky J., Hodis E., Canner D., Decatur W. A., Oberholser K., Martz E., Berchanski A., Harel M., & Sussman J. L. (2011) Proteopedia: A status report on the collaborative, 3D web-encyclopedia of proteins and other biomolecules. *Journal of Structural Biology*, 175(2), 244–252. https://doi.org/10.1016/j.jsb.2011.04.011
Rose A.S., Bradley A.R., Valasatava Y., Duarte J.M., Prlić A., Rose P.W. (2018) NGL viewer: Web-based molecular graphics for large complexes. *Bioinformatics*, 34(21), 3755–3758. doi.org/10.1093/bioinformatics/bty419
Samin H., & Azim T. (2019) Knowledge Based Recommender System for Academia Using Machine Learning: A Case Study on Higher Education Landscape of Pakistan. *IEEE Access*, 7, 67081–67093. https://doi.org/10.1109/ACCESS.2019.2912012
San Juan A. A. (2007) Structural investigation of PAP derivatives by CoMFA and CoMSIA reveals novel insight towards inhibition of Bcr-Abl oncoprotein. *Journal of Molecular Graphics and Modelling*, 26(2), 482–493. https://doi.org/10.1016/j.jmgm.2007.03.001
Sbai A., Bouachrine M. (2022) 3D-QSAR, molecular docking, molecular dynamic simulation, and ADMET study of bioactive compounds against candida albicans. *Moroccan Journal of Chemistry*, 10, 523-541. https://doi.org/10.48317/IMIST.PRSM/MORJCHEM-V10I3.33141
Shagufta Kumar A., Panda G., & Siddiqi M. I. (2007) CoMFA and CoMSIA 3D-QSAR analysis of diaryloxy-methano-phenanthrene derivatives as anti-tubercular agents. *Journal of Molecular Modeling*, 13(1), 99–109. https://doi.org/10.1007/s00894-006-0124-0
Sherry S. T. (2001) dbSNP: The NCBI database of genetic variation. *Nucleic Acids Research*, 29(1), 308–311. https://doi.org/10.1093/nar/29.1.308
Tabti K., Elmchichi L., Sbai A., Maghat H., Bouachrine M., Lakhlifi T., Ghosh A. (2022) In silico design of novel PIN1 inhibitors by combined of 3D-QSAR, molecular docking, molecular dynamic simulation and ADMET studies. *Journal of Molecular Structure,* 1253, 132291, doi.org/10.1016/j.molstruc.2021.132291
Tabti K., El Mchichi L., Moukhliss Y., Singh G., Sbai A., maghat H., bouachrine M., Lakhlifi T. (2022). CoMFA Topomer, CoMFA, CoMSIA, HQSAR, docking molecular, dynamique study and ADMET study on phenyloxylpropyl isoxazole derivatives for coxsackie virus B3 virus inhibitors activity, Mor. J. Chem., 10, 703-725, https://doi.org/10.48317/IMIST.PRSM/morjchem-v10i4.34319
Umair S., Bouchet C., Palevich N., & Simpson H. (2021) Teladorsagia circumcincta 1,6-Bisphosphate Aldolase: Molecular and Biochemical Characterisation, Structure Analysis and Recognition by Immune Hosts. *Parasitologia*, 1(1), 1–11. https://doi.org/10.3390/parasitologia1010001
Veber D. F., Johnson S. R., Cheng H.Y., Smith B. R., Ward K. W., & Kopple K. D. (2002) Molecular Properties That Influence the Oral Bioavailability of Drug Candidates. *Journal of Medicinal Chemistry*, 45(12), 2615–2623. https://doi.org/10.1021/jm020017n
Wang F., Yang W., Li R., Sui Z., Cheng G., & Zhou B. (2021) Molecular description of pyrimidine-based inhibitors with activity against FAK combining 3D-QSAR analysis, molecular docking and molecular dynamics. *Arabian Journal of Chemistry,* 14(6), 103144. https://doi.org/10.1016/j.arabjc.2021.103144
Wang J., Chen W., Zhong H., Luo Y., Zhang L., He L., Wu C., & Li L. (2021) Identify of promising isoquinolone JNK1 inhibitors by combined application of 3D-QSAR, molecular docking and molecular dynamics simulation approaches. *J. Molec. Struc.*, 1225, 129127. doi:10.1016/j.molstruc.2020.129127
Xin Y., Zhou S., Wang H., Hu B., Zhang Z., Wang J., & Sun T. (2021) Comprehensive structure–activity relationship (SAR) investigation of C -aryl glycoside derivatives for the development of SGLT1/SGLT2 dual inhibitors. *New Journal of Chemistry*, 45(31), 14193–14210. https://doi.org/10.1039/D1NJ02510D